

High contrast homeotropic alignment of difluorotolane liquid crystals

CHIEN-HUI WEN, SEBASTIAN GAUZA, JUN LI, HAYING WANG and SHIN-TSON WU*

College of Optics and Photonics, University of Central Florida, Orlando, FL 32816, USA

(Received 23 January 2005; accepted 2 February 2005)

High contrast and excellent homeotropic alignment of high birefringence ($\Delta n \sim 0.3$) and negative dielectric anisotropy difluorotolane liquid crystals were demonstrated using long chain alcohol evaporated SiO_2 inorganic layers and buffed polyimide layers. The addition of 5–10% isothiocyanatotolane not only improves the contrast ratio but also enhances the figure-of-merit. A disadvantage is the increased threshold voltage.

1. Introduction

Homeotropic alignment [1, 2] provides an excellent contrast ratio between crossed polarizers for normally incident light, and this contrast ratio is insensitive to the incident light wavelength, liquid crystal (LC) cell gap, and operating temperature [3]. Therefore, it is a favourable choice for projection and direct view displays. To realize useful electro-optic effects using a longitudinal electric field, homeotropic cells require a negative dielectric anisotropic LC mixture, i.e. $\Delta\epsilon = \epsilon_{\parallel} - \epsilon_{\perp} < 0$. For active matrix displays, high resistivity is another crucial requirement in order to obtain a high voltage-holding ratio and avoid image flickering. To achieve high resistivity, fluorinated compounds are commonly used [4, 5].

For infrared applications of LCs [6], the role of high birefringence and low viscosity becomes even more important because of the longer wavelength and reduced birefringence [7]. To obtain high birefringence, large negative $\Delta\epsilon$ and high resistivity, laterally (2,3) difluorinated tolane [8] or terphenyl [9, 10] LCs are natural choices. The effective dipole moment of the lateral 2,3-difluoro compounds is nearly perpendicular to the principal molecular axis. Thus, from mean field theory [11], these compounds should have a large but negative dielectric anisotropy. However, the difluorotolane and terphenyl mixtures are very difficult to align in a homeotropic cell, leading to a low contrast ratio. Without good alignment, the advantages of homeotropic cells are in vain.

Several methods for achieving homeotropic alignment have been developed [12, 13]. Among them, mechanical rubbing and sputtered SiO_2 [14–16] are most commonly

used because they can produce a stable pretilt angle. With these methods, however, aligning the laterally difluorinated tolane mixtures remains a difficult task.

In this study, we investigated two types of homeotropic cell: buffed polyimide (PI) layers and long chain ($\text{C}_{18}\text{H}_{37}\text{OH}$) alcohol evaporated inorganic SiO_2 layers for aligning the difluorotolane mixtures. For simplicity, we abbreviate the long chain alcohol evaporated SiO_2 cell as LA- SiO_2 cell. For these studies, we formulated two negative $\Delta\epsilon$ LC mixtures, designated as UCF-N3 and -N4, using difluorotolanes. Although the LA- SiO_2 cells align both mixtures well, the SiO_2 sputtering process requires a relatively expensive vacuum system so that the LC panel size is limited by the chamber size. Therefore, the sputtering method is more suitable for small display panels, such as liquid crystal-on-silicon [17]. For large panel direct view displays, buffed polyimide is simpler and more practical. In this work, we found that the doping of 5–10 wt % of a positive $\Delta\epsilon$ compound in to UCF-N3 and -N4 mixtures greatly improves the LC alignment quality of PI cells. Thus, PI cells can be used for aligning difficult laterally difluorinated tolane mixtures.

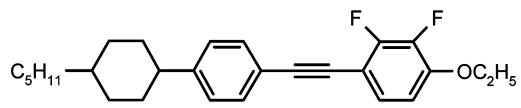
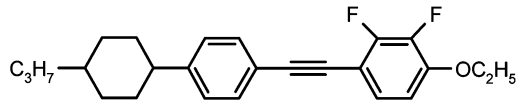
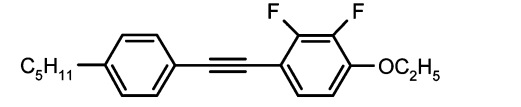
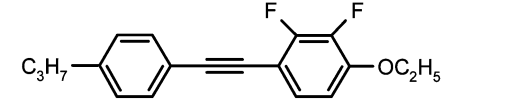
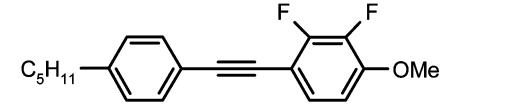
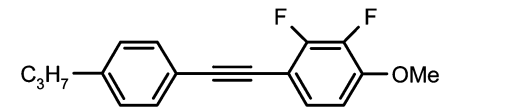
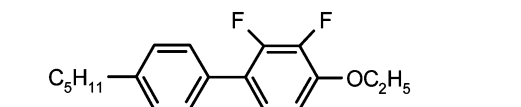
2. Sample preparations

2.1. LC mixtures

Table 1 lists the compositions of UCF-N3 and -N4 mixtures. The major components of these mixtures are 2,3-difluorotolanes. Besides these two host mixtures, we also studied the effect of dopant in enhancing the homeotropic alignment quality. Three isothiocyanato (NCS) tolane [18, 19] dopants were investigated. Their molecular structures and phase transition temperatures are shown in table 2. PTP-2NCS exhibits a monotropic

*Corresponding author. Email: swu@mail.ucf.edu

Table 1. Compositions of UCF-N3 and UCF-N4 LC mixtures.

LC component	Wt% of UCF-N3	Wt% of UCF-N4
	18	19.1
	20	15
	21	19.4
	36	14.3
	0	18.8
	0	9.5
	5	3.9

nematic phase, while CPTP-4NCS exhibits an enantiotropic nematic phase, but with a relatively high melting temperature; the third dopant PTP-3ONCS has no LC phase, its melting point is also quite high because of the alkoxy group.

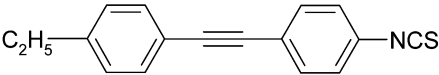
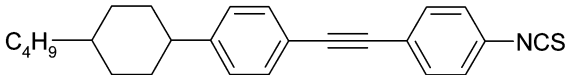
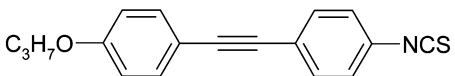
We doped 5, 10, and 15 wt% of these three compounds into the UCF-N3 and -N4 host mixtures. Table 3 gives the abbreviations and phase transition temperatures of these mixtures. We used differential scanning calorimetry (DSC; TA-100) to determine melting and clearing temperatures. Due to the relatively high melting temperatures of these NCS-tolane dopants, the solubility is limited to ~10%; the 15% mixtures crystallize at room temperature.

2.2. Cell preparation

To prepare the PI cells, we spin-coated a commercial polyimide SE-1211 (from Nissan Chemicals) onto the ITO (indium tin oxide)-glass substrates, baked the substrates at 80°C for 5 min and then 180°C for 1 h. We then gently rubbed the ITO-glass with cloth in antiparallel directions; the rubbing-induced pretilt angle was about 87°.

To prepare the LA-SiO₂ cells, we sputtered a thin SiO₂ layer onto the ITO-glass substrates and then evaporated C₁₈H₃₇OH alcohol onto the SiO₂ layer to form a monolayer, as previously reported [14]. The pretilt angle was about 88.5°.

Table 2. Molecular structures and their melting and clearing temperatures of the three positive dopants used in this study.

Positive compound	Molecular structure	Melting point/°C	Clearing point/°C
PTP-2NCS		95.9	87.1
CPTP-4NCS		106.9	257.5
PTP-3ONCS		125.3	125.3

3. Measurements and results

3.1. LC alignments

The alignment capabilities of the LA-SiO₂ and buffed PI cells were first compared. We measured the voltage-dependent transmittance (V - T) curves of both cells filled with UCF-N3 mixture; figure 1 plots the measured results at $\lambda=633$ nm. From figure 1, the voltage-off state of the PI cell ($d\sim 5.2$ μm) has $\sim 2\%$ light leakage and, moreover, its threshold behaviour is smeared. These phenomena imply that the pretilt angle of the cell is too large ($>10^\circ$). The detailed mechanism responsible for the observed large pretilt angle is not yet completely understood, but is speculated to involve molecular interactions between the difluoro group and the rubbed polyimide layer. On the other hand, the LA-SiO₂ cell

($d=3.7$ μm) aligns UCF-N3 quite well; the voltage-off state is very dark and the threshold sharp. The evaporated long chain alcohol molecules were adsorbed onto the SiO₂ surface, serving as a monolayer for aligning the difluorinated molecules. As a result, an excellent homeotropic alignment is achieved.

In figure 1, several transmission cycles are seen because the phase retardation ($\delta=2\pi d\Delta n/\lambda$) of the homeotropic LC cell is large. For display applications, we only need $\delta\sim 1.2\pi$. Thus, a thinner cell gap can be used for achieving a faster response time.

Although the LA-SiO₂ cell aligns the difluoro mixtures well, its fabrication process requires vacuum so that the panel size is limited. The buffing method is more convenient and less expensive for large LC panels. To improve the alignment capability of the rubbed PI

Table 3. Melting and clearing temperatures of the UCF mixtures with and without dopants.

Code	Base mixture	Dopant	Wt % of dopant	$T_m/^\circ\text{C}$	$T_J/^\circ\text{C}$
UCF-N3			0	-51.8	113.8
UCF-N3a	UCF-N3	PTP-2NCS	5	-51.8	110.2
UCF-N3b			10	-52.0	107.0
UCF-N3c			15	44.2	103.5
UCF-N4			0	-51.8	108.5
UCF-N4a	UCF-N4	PTP-2NCS	5	-51.8	105.0
UCF-N4b			10	-52.4	101.2
UCF-N4c			15	43.5	97.4
UCF-N4d	UCF-N4	CPTP-4NCS	5	-51.2	113.8
UCF-N4e			10	-50.3	122.1
UCF-N4f	UCF-N4	PTP-3ONCS	5	-51.2	107.5
UCF-N4g			10	-50.9	106.5

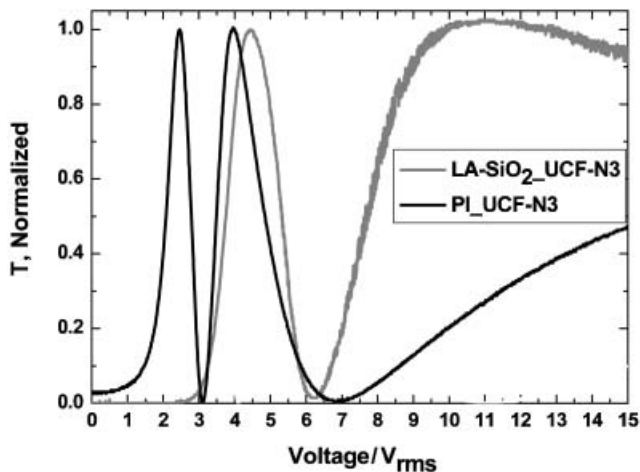


Figure 1. Voltage-dependent transmittance of a homeotropic cell between crossed polarizers. The black line represents UCF-N3 in a buffed PI cell. The grey line represents UCF-N3 in the LA-SiO₂ cell. $\lambda=633$ nm, $T=23^\circ\text{C}$.

cells, we doped some positive compounds, as listed in table 4, into the host UCF-N3 and -N4 mixtures. Figure 2 plots the V - T curves of the rubbed PI cells filled with UCF-N3, -N3a, and -N3b. The polarizers are crossed and the on-state LC directors are at 45° with respect to the polarizer's optical axis. In figure 2, the data for UCF-N3 is included as a benchmark for comparison. Doping 5% of PTP-2NCS (sample UCF-N3a) suppresses the dark state light leakage noticeably, but this is still not perfect as shown by the dashed lines. Increasing the PTP-2NCS to 10% (sample UCF-N3b) leads to an excellent dark state and sharp threshold (grey line). A shortcoming in doping a positive $\Delta\epsilon$ compound into a negative host mixture is that the effective $|\Delta\epsilon|$ is decreased so that the threshold voltage is increased.

3.2. Threshold voltage

The threshold voltage of a homeotropic cell is related to $\Delta\epsilon$ as $V_{\text{th}} = \pi(K_{33}/\epsilon_0\Delta\epsilon)^{\frac{1}{2}}$. While deriving the expression

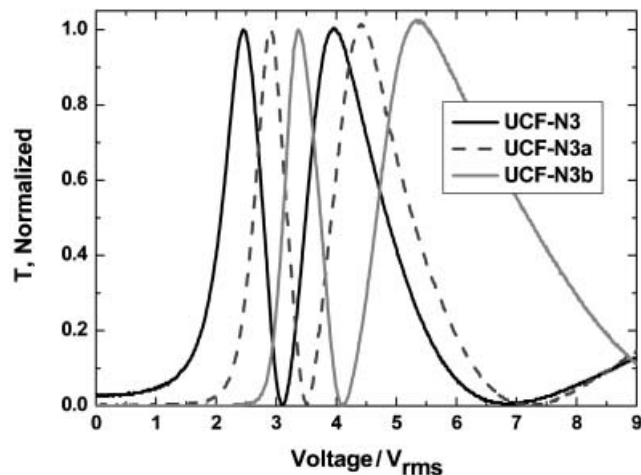


Figure 2. Voltage-dependent transmittance of UCF-N3 containing 0% (black line), 5% (dashed line) and 10% (grey line) of PTP-2NCS. The transmittance was measured using a homeotropic PI alignment cell between two crossed polarizers at $\lambda=633$ nm. Cell gap $d\sim 5.2$ μm .

for the threshold voltage, the pretilt angle is assumed to be zero. However, in reality the LC cell always has a small pretilt angle in order to guide the relaxation direction of the LC directors. With this pretilt angle, the threshold would not be perfectly sharp. For the same LC material employed, a larger pretilt angle cell would result in a lower apparent threshold voltage. The PTP-2NCS compound we used has a relatively large and positive dielectric anisotropy ($\Delta\epsilon\sim 12$). Thus, the addition of 10% of PTP-2NCS into the UCF-N3 host will reduce the effective $\Delta\epsilon$ of the mixture and result in an increased threshold voltage. From figure 2, the V_{th} of UCF-N3b is $\sim 2.7V_{\text{rms}}$, which is approximately the same as that of UCF-N3 in the LA-SiO₂ cell. UCF-N3 has a larger, but negative, $\Delta\epsilon$ than UCF-N3b; in theory, the UCF-N3 cell should have a lower threshold voltage. However, the LA-SiO₂ cell has a smaller pretilt angle ($\sim 1.5^\circ$) than the rubbed PI cell ($\sim 3^\circ$); thus, its apparent threshold voltage is about the same as that for UCF-N3b in the rubbed PI cell.

Table 4. Birefringence (Δn), visco-elastic coefficient (γ_1/K_{33}), figure-of-merit (FoM), and dielectric anisotropy ($\Delta\epsilon$) of the UCF negative LC mixtures containing 5% and 10% of positive compounds.

Mixtures	Δn	γ_1/K_{33}	FoM	$\Delta\epsilon$
UCF-N3a	0.30	19.0	4.73	-4.3
UCF-N3b	0.31	13.0	7.39	-3.3
UCF-N4a	0.29	14.5	5.84	-4.4
UCF-N4b	0.30	13.2	6.82	-3.2
UCF-N4d	0.29	18.8	4.57	-4.7
UCF-N4e	0.31	17.4	5.56	-3.4
UCF-N4f	0.30	16.7	5.42	-4.3
UCF-N4g	0.31	14.9	6.45	-3.2

Figure 3 depicts the V - T curves between crossed polarizers of the buffed PI cells filled with UCF-N4, -N4a, -N4d and -N4f. The cell gap is $d \sim 5.2 \mu\text{m}$ and $\lambda = 633 \text{ nm}$. The UCF-N4 cell has $\sim 1\%$ light leakage in the voltage-off state and its threshold is not as sharp as it should be. Adding 5% of PTP-2NCS, CPTP-4NCS or PTP-3ONCS into UCF-N4 greatly improves the dark state and threshold behaviour. The V - T curves of UCF-N4a, -N4d and -N4f almost overlap with each other. The transmittance reaches ~ 0 and 100% at the voltage-off and -on states, respectively. From figure 3, the positive compounds indeed help the host difluorotolane mixture to align well in the rubbed PI cells.

3.3. Contrast ratio

We also measured the contrast ratios of the cells shown in figure 3. The contrast ratio of UCF-N4 in the rubbed PI cell is $\sim 100:1$, which indicates that the alignment quality is not perfect. For the mixtures containing 5% and 10% of PTP-2NCS in a rubbed PI cell, their dark state transmittance is limited by the crossed polarizers. The estimated contrast ratio exceeds 10000:1 for the He-Ne laser beam employed.

3.4. Refractive indices

We also measured the n_e and n_o of UCF-N3b at six visible wavelengths ($\lambda = 450, 486, 546, 589, 633$ and 656 nm) and different temperatures. We used a multi-wavelength Abbe refractometer (Atago DR-M4) to measure the n_e and n_o of the LC mixture. The temperature of the Abbe refractometer was controlled by a circulating constant temperature bath (Atago

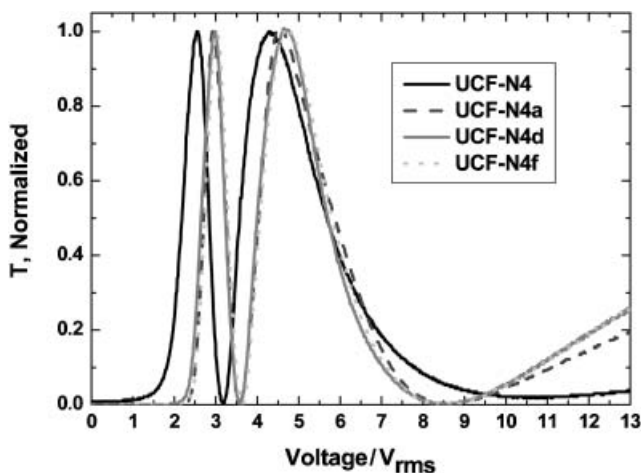


Figure 3. Voltage-dependent transmittance of UCF-N4 containing 5% of positive compound. Black, black dashed, grey and dotted light grey lines represent UCF-N4, UCF-N4a, -N4d, and -N4f, respectively. $\lambda = 633 \text{ nm}$ and $d \sim 5.2 \mu\text{m}$.

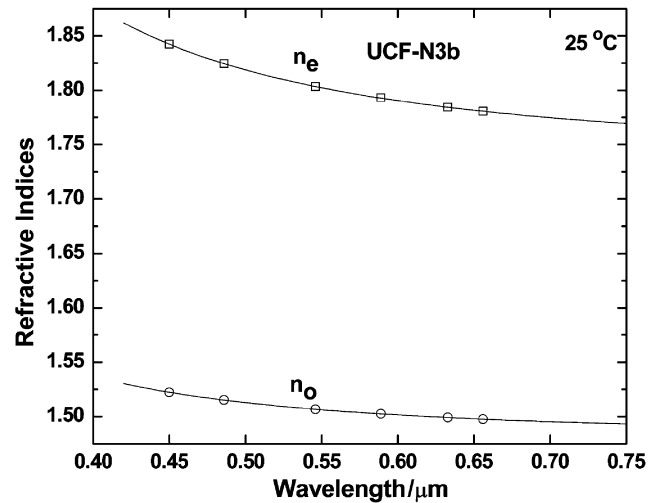


Figure 4. Wavelength-dependent refractive indices of UCF-N3b at $T = 25^\circ\text{C}$. Dots are experimental data and solid lines are fittings using equations (1) and (2) for n_e and n_o , respectively.

Model 60-C3). Results for the wavelength- and temperature-dependent refractive indices of UCF-N3b are plotted in figures 4 and 5, respectively. For the wavelength-dependent refractive indices measurements, the temperature was fixed at $T = 25^\circ\text{C}$.

The solid lines in figure 4 represent fittings with the extended Cauchy equations [20, 21]:

$$n_e = A_e + B_e/\lambda^2 + C_e/\lambda^4 \quad (1)$$

$$n_o = A_o + B_o/\lambda^2 + C_o/\lambda^4 \quad (2)$$

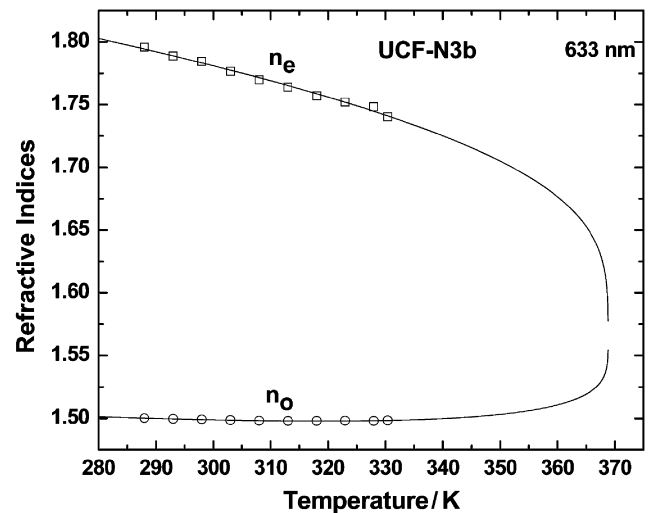


Figure 5. Temperature-dependent refractive indices of UCF-N3b at $\lambda = 633 \text{ nm}$. Dots are experimental data and solid lines are fittings with theory.

In equations (1) and (2), $A_{e,o}$, $B_{e,o}$ (in units of μm^2), and $C_{e,o}$ (in units of μm^4) are called Cauchy coefficients for the extraordinary and ordinary refractive indices. From fittings, the six Cauchy coefficients are obtained as: $[A_e, B_e, C_e]=[1.7372, 0.0165, 0.0010]$, and $[A_o, B_o, C_o]=[1.4802, 0.0066, 0.0004]$. From figure 4, the agreement between experiment and theory is excellent. As the wavelength increases, n_e decreases much more rapidly than n_o . Once the Cauchy coefficients are known, we can extrapolate the refractive indices of UCF-N3b to any required wavelength. For example, at $\lambda=10.6\mu\text{m}$ the extrapolated $n_e=1.7374$, $n_o=1.4803$, and $\Delta n=0.2571$ at $T=25^\circ\text{C}$.

In figure 5, we plot the temperature-dependent refractive indices of UCF-N3b at $\lambda=633\text{ nm}$. Solid lines represent fittings with the following simple expressions [22]:

$$n_e = \langle n \rangle + \frac{2}{3} \Delta n \quad (3)$$

$$n_o = \langle n \rangle - \frac{1}{3} \Delta n \quad (4)$$

where $\langle n \rangle$ represents the average refractive index and Δn is the LC birefringence. The average refractive index decreases linearly with temperature as $\langle n \rangle = A - BT$ and birefringence decreases with temperature as $\Delta n = (\Delta n)_o (1 - T/T_o)^\beta$; where A , B , $(\Delta n)_o$ and β are material parameters [22, 23]. From equation (3), the right-hand two terms both decrease as the temperature increases; thus, n_e decreases monotonously with increased temperature. That is to say, the temperature derivative of n_e ($\partial n_e / \partial T$) is always negative. However, for $\partial n_o / \partial T$ there exists a cross-over temperature T_o [24] where $\partial n_o / \partial T = 0$. Below T_o , n_o decreases with increased temperature, whereas above T_o , n_o increases with increasing temperature.

4. Discussion

In addition to enabling excellent alignment, doping with 5–10% of a NCS-tolane leads to a higher birefringence and lower viscoelastic coefficient. The birefringence of the NCS-tolane is around 0.38, which is higher than that of the negative difluorotolanes. Moreover, the NCS group possesses a low viscosity; thus, the doped mixtures show an improved figure-of-merit.

Figure 6 plots the temperature-dependent figure-of-merit of UCF-N3b and a Merck high birefringence negative $\Delta\epsilon$ LC mixture MLC-4850. Dots and triangles represent the measured data for UCF-N3b and MLC-4850, respectively, while the solid line represents the fitting curves using the following equation [25]:

$$FoM \sim (\Delta n)_o^2 (1 - T/T_c)^{3\beta} \exp(-E/kT) \quad (5)$$

where $(\Delta n)_o$ is the birefringence when $T=0$, E is the

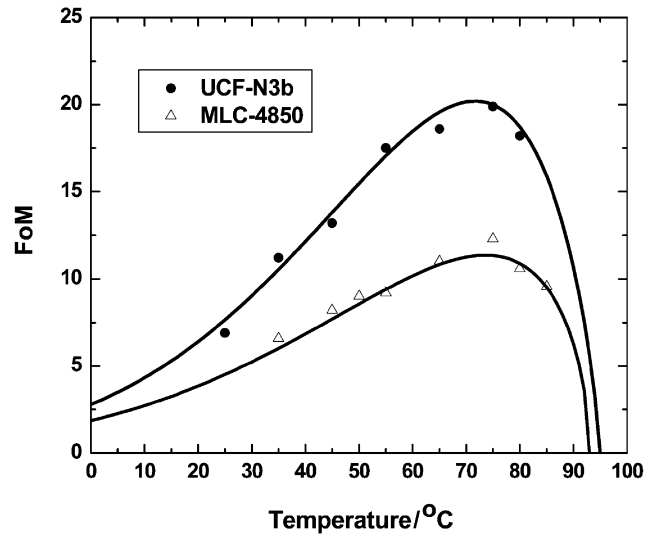


Figure 6. Temperature dependent figure-of-merit ($\mu\text{m}^2\text{ ms}^{-1}$) of UCF-N3b (circles) and MLC 4850 (triangles). Solid lines are fittings to the experimental data.

activation energy of the rotational viscosity, k is the Boltzmann constant, and the exponent $\beta \sim 0.25$ is not too sensitive to the LC structure. As the temperature increases, the FoM increases gradually. At the optimal operating temperature ($T_{op} \sim 75^\circ\text{C}$), FoM reaches a maximum value, which is $20\mu\text{m}^2\text{ ms}^{-1}$ for UCF-N3b and $\sim 10\mu\text{m}^2\text{ ms}^{-1}$ for MLC-4850. The peak FoM of UCF-N3b is almost twice that of MLC-4850.

5. Conclusion

We have compared the homeotropic alignment capability of LA-SiO₂ and rubbed PI cells for high birefringence difluorotolane LC mixtures. The LA-SiO₂ cells exhibit an excellent dark state and sharp threshold. However, the PI cells do not align the difluorotolane mixtures well. On adding a few percent of NCS-tolane compound to the host negative difluorotolane mixtures, the buffed PI cells exhibit an excellent homeotropic alignment. Adding the positive NCS tolans has advantages and disadvantages. The alignment is excellent and the figure-of-merit increases; however, the threshold voltage is increased because of the reduced dielectric anisotropy.

References

- [1] M.F. Schiekel, K. Fahrenschon. *Appl. Phys. Lett.*, **19**, 391 (1971).
- [2] F.J. Kahn. *Appl. Phys. Lett.*, **22**, 386 (1973).
- [3] S.T. Wu, D.K. Yang. *Reflective Liquid Crystal Displays*. Wiley, New York (2001).
- [4] V. Reiffenrath, U. Finkenzeller, E. Poetsch, B. Rieger, D. Coates. *Proc. SPIE*, **1257**, 84 (1990).

- [5] Y. Goto, T. Ogawa, S. Sawada, S. Sugimori. *Mol. Cryst. liq. Cryst.*, **209**, 1 (1991).
- [6] S.T. Wu, U. Efron, L.D. Hess. *Appl. Phys. Lett.*, **44**, 1033 (1984).
- [7] S.T. Wu. *Phys. Rev. A*, **33**, 1270 (1986).
- [8] S.T. Wu, C.S. Hsu, J.M. Chen. *Mol. Cryst. liq. Cryst.*, **304**, 441 (1997).
- [9] G.W. Gray, M. Hird, K.J. Toyne. *Mol. Cryst. liq. Cryst.*, **204**, 43 (1991).
- [10] D. Pauluth, K. Tarumi. *J. mater. Chem.*, **14**, 1219 (2004).
- [11] W. Maier, G.Z. Meier. *Z. Naturforsch A*, **16**, 262 (1961).
- [12] J. Cognard. *Mol. Cryst. liq. Cryst. Suppl.*, **1**, 1 (1982).
- [13] J.L. Janning. *Appl. Phys. Lett.*, **21**, 173 (1972).
- [14] A.M. Lackner, J.D. Margerum, L.J. Miller, W.H. Smith. *Proc. SID*, **31**, 321 (1990).
- [15] W.H. Smith, H.L. Garvin, K. Robinson, L.J. Miller. US patent 5 620 755 (1997).
- [16] M. Lu, K.H. Yang, T. Nakasogi, S.J. Chey. *SID Dig.*, **31**, 446 (2000).
- [17] H. Kurogane, K. Doi, T. Nishihata, A. Honma, M. Furuya, S. Nakagaki, I. Takanashi. *SID Dig.*, **29**, 33 (1998).
- [18] S. Gauza, H. Wang, C.H. Wen, S.T. Wu, A.J. Seed, R. Dabrowski. *Jpn. J. appl. Phys.*, **42**, 3463 (2003).
- [19] A. Spadło, R. Dąbrowski, M. Filipowicz, Z. Stolarz, J. Przedmojski, S. Gauza, Y.H. Fan, S.T. Wu. *Liq. Cryst.*, **30**, 191 (2003).
- [20] S.T. Wu, C.S. Wu, M. Warengem, M. Ismaili. *Opt. Eng.*, **32**, 1775 (1993).
- [21] J. Li, S.T. Wu. *J. appl. Phys.*, **95**, 896 (2004).
- [22] J. Li, S. Gauza, S.T. Wu. *J. appl. Phys.*, **96**, 19 (2004).
- [23] I. Haller. *Prog. solid state Chem.*, **10**, 103 (1975).
- [24] J. Li, S. Gauza, S.T. Wu. *Opt. Express*, **12**, 2002 (2004).
- [25] S.T. Wu, A.M. Lackner, U. Efron. *Appl. Opt.*, **26**, 3441 (1987).